

# Learning to Recognize Spatial Configurations of Objects with Graph Neural Networks

Laetitia Teodorescu<sup>1</sup> Katja Hofmann<sup>2</sup> Pierre-Yves Oudeyer<sup>3</sup>

## Abstract

Deep learning algorithms can be seen as compositions of functions acting on learned representations encoded as tensor-structured data. However, in most applications those representations are monolithic, with for instance one single vector encoding an entire image or sentence. In this paper, we build upon the recent successes of Graph Neural Networks (GNNs) to explore the use of graph-structured representations for learning spatial configurations. Motivated by the ability of humans to distinguish arrangements of shapes, we introduce two novel geometrical reasoning tasks, for which we provide the datasets. We introduce novel GNN layers and architectures to solve the tasks and show that graph-structured representations are necessary for good performance.

## 1. Introduction

An artificial agent acting on the world has to represent its sensory inputs in an adequate way, providing sufficient information and bias for it to efficiently compute adequate responses to its inputs and learn from data. A good design principle for this representation is factorisation: the fact that the agent is able to represent its sensory inputs as a collection of (hierarchically structured) independent elements that can be processed separately and in parallel (Pylyshyn, 2007). This endows the agent’s computation with a useful locality property: if each element of the representation corresponds to one element of the environment, changing only one constitutive element of the outside scene only changes the corresponding element of the inside representation, allowing the agent to isolate the source of change and the result of its actions; it also provides a straightforward way to generalize by applying some function learned on one entity to other entities.

<sup>1</sup>Inria, France <sup>2</sup>Microsoft Research Cambridge, UK  
<sup>3</sup>Inria, France. Correspondence to: Laetitia Teodorescu  
<maria.teodorescu@inria.fr>.

<sup>2</sup>Similar collections are Configurations 1 and 4

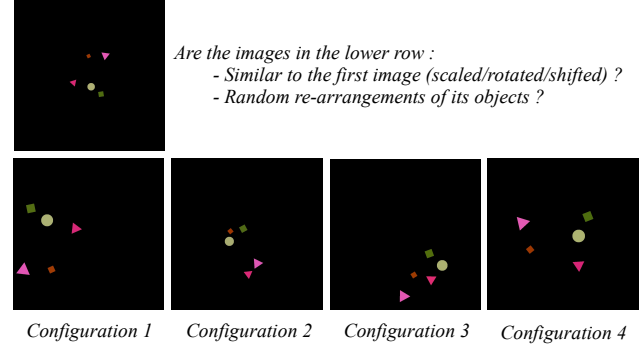


Figure 1. Visual illustration of the task defined in this work. Which of the lower examples are positive samples, and which are negative? Answers in footnote <sup>2</sup>

However, sets of objects are an insufficient description of the world for most purposes. In general, to accurately describe and predict the world one must not only consider its constitutive elements but also how they relate to each other: consider, e.g., that predicting the motion of objects in a many-bodied problem requires information about the pairwise distances between objects, or consider the fact that judging whether a tower of blocks is stable or will fall is a decision that is to be made by relating the different constituent elements of the tower one to the other. The notion of a tower itself is best described as a particular configuration of individual blocks. Thus, such problems cannot be solved by representing the bodies as an unordered set and applying functions to each element of the set independently. When using an object-centric representation of the world, problems involving relational information are ubiquitous (physical stability and motion (Hamrick et al., 2018b), intuitive psychology (Lake et al., 2016); temporal chains of events; it is also evidenced by language, which is an elaborate way of relating individual concepts). An adequate representation for those kinds of problems, preserving the aforementioned property of locality while explicitly encoding the relationships between objects is a graph where the nodes represent the constitutive elements of the world and the edges represent the links between objects.

In recent years there has been increasing interest in methods for deep learning on graph-structured data, using a class of networks called Graph Neural Networks (GNNs) (Scarselli et al., 2009; Kipf & Welling, 2016; Battaglia et al., 2018). These methods operate on an input graph where each node has an associated node feature, and updates them according to a message-passing scheme where each node communicates along the edges of the graph with every other node of its neighborhood. A GNN can output the updated node features that can be used for node-wise prediction, or can output a graph-wide feature that can be used for graph prediction. These methods have successfully been used to learn physical simulation, to classify graph-structured data, to generate graphs matching the statistics of a given dataset, and to planning and control. While these applications showcase the power of GNNs in a vast range of settings, there remain important questions as to the power of GNNs to solve global recognition tasks in scenes an agent might encounter.

Spatial reasoning skills are crucial for agents that need to interact with objects in the physical world. In this work, we propose two naturally-occurring spatial reasoning tasks that mimic the problems an agent will be faced when observing collections of objects from different points of view (see Figure 1 for a visual example). We consider a configuration of objects embedded in 2d space, and learn to predict whether it is a scaled, translated and/or rotated version of a reference configuration. More specifically, we define the following two tasks. In the first, the model is always presented the same set of objects and has to decide if the configuration is the same as a constant reference. In the second one, the model has to learn to relate two sets of objects, and say whether they are similar or not. These settings are representative of a larger class of problems of spatial reasoning : for instance, an RL agent that needs self-supervision signals to decide when two scenes are the same or not and when no external guidance from humans or external labels are provided (with the aim to train a goal achievement function like contrastive networks), and to our knowledge no work has studied how GNNs can solve them.

Confronted with these problems, we hypothesise that leveraging the message-passing computation allowed by GNNs is key for efficient learning and generalization. We then ask what kind and amount of message passing is necessary for good performance, and compare fully-connected message-passing to a form of centralized message-passing we call Recurrent Deep Sets (RDS), and to models based on Deep Sets (Zaheer et al., 2017) that contain no message passing.

In this work, our main contribution is showing that message passing computation is key to learning on the configuration recognition task and especially on the configuration comparison task, suggesting that the underlying graph supporting the representation of the data is necessary for spatial

reasoning tasks. To do this, we :

- Introduce two spatial reasoning tasks, along with their associated datasets;
- Compare the performance of a set of GNN layers (Message-Passing GNN and our Recurrent Deep Sets) and architectures on these two tasks.

## 2. Related Work

### 2.1. Graph Neural Networks

This research extends the recent line of work on neural networks that operate on graph-structured input. Seminal work (Gori et al., 2005; Scarselli et al., 2009) involved updating the representations of nodes using a contraction map of their local neighborhood until convergence, a computationally expensive process. Follow-up work alleviated this, by proposing neural network models where each layer performs an update of node features based on the previous features and the graph’s adjacency matrix, and several such layers are stacked to produce the final output. Notably, Graph Convolutional Networks (GCNs) (Kipf & Welling, 2016) (Defferrard et al., 2016) (Bruna et al., 2014), in their layers, use a linear, first-order approximation of spectral graph convolution and proved effective in several domains (Duvenaud et al., 2015). However, these works have focused on working on large graphs where the prediction at hand depends on its connectivity structure, and the GCN can learn to encode the structure of their k-hop neighborhoods (for k computation steps). In our case there are a lot less objects, and the precise connectivity is irrelevant since we create our graphs without any prior knowledge pertaining to the objects.

A different class of networks has been proposed to more explicitly model an algorithm of message-passing between the nodes of a graph, using the edges of the graph as the underlying structure on which to propagate information. This is the class of model that we consider in this work, because of their flexibility and generality. A variant of this was first proposed to model objects and their interactions (Battaglia et al., 2016; Santoro et al., 2017) by explicitly performing neural computation on pairs of objects. The full message-passing framework was introduced in (Gilmer et al., 2017) for supervised learning on molecules, and was expanded in (Battaglia et al., 2018), which provided a unifying view.

A line of theoretical work has focused on proving the representational power of GNNs. Xu et al. (2018) introduced a simple model that is provably more powerful than GCNs, and universality of approximation theorems for permutation invariant (Maron et al., 2019) and permutation equivariant (Keriven & Peyré, 2019) functions of nodes of a graph have also derived recently. However, the models constructed in these proofs are theoretical and cannot be tractably imple-

mented. In this work, we provide empirical evidence that Message-Passing GNNs have the representational power to deal with spatial similarity recognition.

Finally, our work relates to recent work on learning distance functions over pairs of graphs (Ma et al., 2019). Recent work (Li et al., 2019b), in a model they call Graph Matching Network, has proposed using a cross-graph node-to-node attention approach for solving the problem, and compared it to an approach without cross-graph attention, that is related to our Graph Embedding architecture. While more effective than the other approach on the set of tasks they considered, it amounts in some sense to breaking the hierarchy of the problem by creating a great graph composed of the two subgraphs. Our work is closely related, because it also pertains to graph comparison, however, our work is distinct from previous work because, in addition to comparing two input graphs, we want to study whether we can condition computation on one graph by an external embedding, here of the other graph.

## 2.2. Graphs as representations

Graph representations are increasingly applied in domains where data is not, at first look, structured as a graph. For instance, in computer vision, representing an image as a scene graph (Johnson et al., 2015; Krishna et al., 2016) allows explicit modelling of semantic information and transfer to downstream tasks such as question answering (Battaglia et al., 2018; Teney et al., 2016; Norcliffe-Brown et al., 2018) (Hudson & Manning, 2019). Scene graph-representations make it possible to apply GNNs to these tasks, an approach that has been proved successful for predicting physical interactions between a set of objects (Battaglia et al., 2016). While the setting of this physical prediction work has similarities to our own setting (a small number of objects in 2d space), the task involves updating the object representations for each object, to get its next position in time, while our work focuses on predicting an output for all objects. We argue that the problem is harder since, in addition to performing operations on the objects our models have to learn to produce a meaningful summary of the information in all objects.

Recent work has also begun using the compositional structure allowed by graph-based representations to inform the behavior of an agent in a reinforcement learning setting, allowing for learning structured world models (Kipf et al., 2019). This graph structure of the state representation has been shown to be crucial in one-shot imitation learning tasks in a robotic setting (Sieb et al., 2019), prediction of the stability of a tower of blocks (Hamrick et al., 2018a) and a block-stacking task (Li et al., 2019a). A key limitation is that approaches developed so far require object identity. We prove our approach to be more general and expect that

reasoning in RL will be an important future application of our models.

## 3. Methods

### 3.1. Spatial configurations of objects

In this work, we consider the problem of learning to recognize whether one spatial configuration of objects is equivalent to another. We define a set of  $n_{obj}$  objects as colored shapes in 2D space, each uniquely characterized by a  $d_x$ -dimensional feature vector composed of a set of discrete features describing its shape, and a set of continuous features describing its size, x-y position, color and orientation. We leave working directly with images for further work, and we note a series of recent interesting work in unsupervised object extraction from images (see (Burgess et al., 2019; Greff et al., 2019; Engelcke et al., 2019)) that could be used as a first feature extraction step.

We define a spatial configuration of objects as a set  $S_1$  of these objects, and we consider the class of all sets of objects  $S$  that can be obtained by applying to  $S_1$  a direct isometry composed with a scaling, up to a perceptive noise factor of  $\varepsilon$  on every feature. (see 1 for a visual example). This defines the equivalence class for the similarity relation, and we define our problem as the problem of learning to disambiguate between members of the class and outside the class.

We decline this problem in two variants, that we explore in the following sections : the first variant sees a different dataset generated for each similarity class, with positive examples similar to a reference configuration, and the negative ones being random re-positionings of objects - the classification problem is to assign correct labels to positive and negative examples. In this first setting, our GNN operates on a single input graph. In the second setting, each example consists of two inputs, which may or may not come from the same class, and the task of our GNN is to learn to label examples of two similar configurations as *True* and other examples as *False*; in this second setting the GNN takes two different configurations as input. The first setting can be seen as training a different model for each class, and the second setting as having a *universal* model that can perform computations that are valid for any input set of objects. We detail the data generation for those two settings and the models in the following sections.

### 3.2. First task: configuration recognition

In our first experiments, we are interested to see if we can find an neural architecture able to learn to recognize one spatial configuration of objects. Based on one reference configuration, randomly generated by sampling  $n$  objects in 2d space, we generate a balanced dataset composed of :

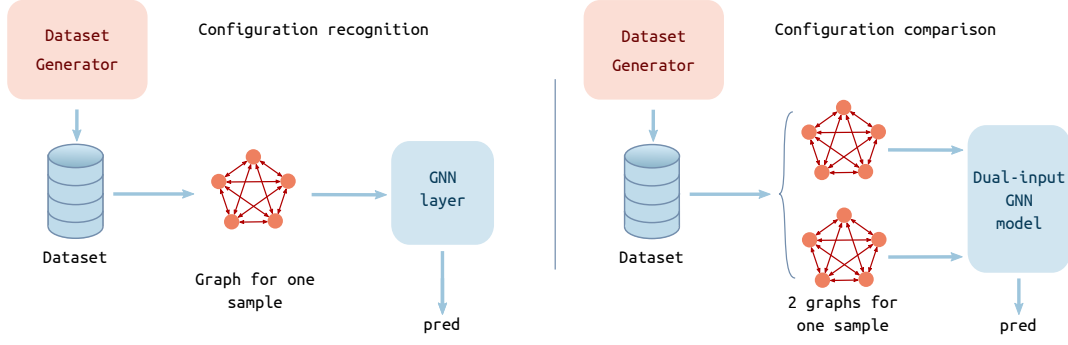


Figure 2. Illustration of our two different settings. For the configuration recognition task, each different sample is associated with a single configuration, and thus gives a single graph as input to our layers. For the configuration comparison task, each sample leads to building two input graphs as input to our architectures.

- **Positive examples** : after applying a small perturbation, quantified by  $\varepsilon$ , to each of the objects in the reference, very slightly changing their color, position, size and orientation, we apply a rotation around the mean position of the configuration with an angle  $\phi \sim \mathcal{U}([0, 2\pi])$ , a scaling, with center the mean position of the configuration and magnitude  $s \sim \mathcal{U}([0.5, 2])$ , and a translation of vector  $t$ ;
- **Negative examples** : these examples are generated by applying a small perturbation to the features of the objects in the reference, and then re-sampling randomly the positions of the objects. While it is, in theory, possible to sample a negative example that is close to the positive class, the probability is very low in practice for numbers of objects  $n \geq 3$ .

We illustrate the experimental setup in figure 2.

This simple setting allows us to isolate how well the model is able to learn as a function of the number of objects  $n_{obj}$ : indeed, the model must make a decision that depends on the relationship between all objects, and for this purpose has to aggregate incoming information from  $n_{obj}$  vectors : when  $n_{obj}$  gets large and the dimension of the embedding vector  $u$  stays constant, information is bound to be lost, and as a consequence the performance is bound to suffer when  $n_{obj}$  gets large enough. This setting also allows us to study the inherent difficulty or easiness of particular datasets, as a function of the diversity of the samples.

### 3.3. Models for configuration recognition

In this section we present our graph creation procedure and a series of GNN layers, that exhibit decreasing connectivity between nodes in their computation : fully-connected, node-to-node communication for the Message-Passing GNN; centralized communication to a central, graph-level feature for

the Recurrent Deep Set. We give a visual comparison of the two layers along with the Deep Set baseline in the Supplementary Material.

#### 3.3.1. GRAPH CREATION

From a set of objects  $S$  we construct a fully-connected, directed graph  $G$  that is used as an input to our GNN. In our work,  $G = (X, A, E, u)$  contains the following information :

- $X \in \mathbb{R}^{n \times d_x}$  is a tensor of node features, containing a vector of dimension  $d_x$  for each of the objects in the scene;
- $A \in \mathcal{M}^{n \times n}$  is the adjacency matrix of the graph;
- $E \in \mathbb{R}^{e \times d_e}$  is a tensor of edge features, also referred to as messages in the rest of this article, labeling each of the  $e$  edges with a  $d_e$ -dimensional vector, and that can be seen as information propagating from the sender node to the receiver node;
- $u$  is a graph-level feature vector, used in the GNN computation to store information pertaining to the whole graph, and effectively used as an embedding of the graph to predict the class of the input.

**Initialization of the graph** : Since our models require an input for  $E$  and  $u$  that is not *a priori* given in the description of the collection of objects, we use a generic initialization scheme :  $u$  is initialized with the mean of all node features, and each edge is initialized with the difference between the features of the sender node and the receiver node.

#### 3.3.2. MESSAGE-PASSING GNN

Our message-passing graph neural network can be seen as a function operating on graph input and producing a graph out-

put:  $GNN : G(X, A, E, u) \rightarrow G'(X', A, E', u')$ , where the dimensionality of the node features, edge features and global features can be changed by the application of this function, but the graph structure itself encoded as the adjacency matrix  $A$  is left unchanged. This GNN layer can then itself be seen as the composition of several functions, each updating a part of the information contained in the graph :

**Message computation** : We denote by  $E_{i \rightarrow j}$  the feature vector of the edge departing from node  $i$  and arriving at node  $j$ ,  $X_i$  the feature vector of node  $i$ , and  $[x||y]$  the concatenation of vectors  $x$  and  $y$ , and by  $MLP$  a multi-layer perceptron. The message passing step is then defined as :

$$E'_{i \rightarrow j} \leftarrow MLP_E([X_i||X_j||E_{i \rightarrow j}||u])$$

At each time step, the message depends on the features of the sender and receiver nodes, the previous message, and the global vector  $u$ .

**Node-wise aggregation** : Once the message along each edge is computed, the model computes the new node features from all the incoming edges. We define by  $\mathcal{N}(j)$  the incoming neighbourhood of node  $j$ , that is, the set of nodes  $i \in [1..n]$  where there exists an edge going from  $i$  to  $j$ . The node computation is then performed as so :

$$X'_j \leftarrow MLP_X\left([X_j||\sum_{i \in \mathcal{N}(j)} E'_{i \rightarrow j}||u]\right)$$

**Graph-wise aggregation** Finally, we update the graph-level feature, that we use as an embedding for classification, and that conditions the first and second time step of computation :

$$u' \leftarrow MLP_u\left([\sum_i X'_i||u]\right)$$

**Prediction** : the final step is passing the resulting vector  $u$  through a final multi-layer perceptron to produce logits for our binary classification problem :

$$out \leftarrow MLP_{out}(u')$$

We use the same dimensionality for the output vectors as for the input vectors of the message computation, node aggregation and graph aggregation, and this allows us to stack  $N$  GNN computations in a recurrent fashion.

### 3.3.3. RECURRENT DEEP SETS

We also introduce, for comparison purposes, a simpler model we term Recurrent Deep Sets (RDS). This method dispenses with the message computation and node aggregation part, and at each step only transforms the node features and aggregates them into the graph feature. This architecture is quite reminiscent of the Deep Set (Zaheer et al., 2017),

to the important difference that the graph-level feature  $u$  is then fed back at the following step by being concatenated to the object feature for the next round of computation. This allows the computation of features for each object to depend on the state of the whole configuration, as summarized in the graph embedding  $u$ . This contrasts with the original Deep Sets, where each object is processed independently. The functional description of this model is thus :

$$\begin{aligned} X'_j &\leftarrow MLP_X([X_j||u]) \\ u' &\leftarrow MLP_u\left([\sum_i X'_i||u]\right) \\ out &\leftarrow MLP_{out}(u') \end{aligned}$$

Note that for this model, there is no need to connect each object to every other object. However, this back-and-forth between node computation and graph aggregation can be interpreted as computing messages between each object and a central node, that represents the information of the whole graph. In this sense, this model can be interpreted as a GNN operating on the star-shaped graph of the union of the set of objects and the central graph-level node. In particular, this means that the resulting model performs a number of computations that scales linearly in the number of nodes, instead of quadratically as is the case for a message-passing GNN on the complete, fully connected graph of objects. While this is an interesting propriety, in practice for a fixed size of  $u$  the number of objects cannot grow arbitrarily large because the success of our models depend on the ability of  $u$  to accurately summarize information which is dependent on all the objects, which becomes difficult as the number  $n$  of objects becomes large.

### 3.4. Second task : comparing configurations

In this section, we describe our second setup. While in the previous setup the model had to learn to recognize a precise configuration, and could for this purpose learn to perform particular computations regardless of the input, we describe a more complex and complete setting where the model has to learn to *compare* two different configurations that are re-drawn for each sample (see Figure for an illustration). In this case, each data sample is composed of two sets of objects that are generated in the following fashion :

- **Positive examples** : we draw the first configuration by randomly sampling the objects' shape, size, color, position and orientation. For obtaining the second configuration, we copy the first one, apply a small perturbation to the features of each object, and apply a random rotation, scaling, and translation to all objects;
- **Negative examples** : we draw the first configuration as above, and for the second one we randomly re-sample

the positions of each object independently, while keeping the other features constant. We finally apply a random rotation, scaling and translation and this gives us our second set of objects.

This task, while being more difficult, is also more general and more realistic : while sometimes an agent may be confronted with numerous repetitions of the same configuration that it has to learn to recognize - for instance, humans become, by extensive exposition, quite proficient at the task of recognizing the special configuration of visual elements that is human faces (Maurer et al., 2002) - but a very common task an intelligent agent will be confronted to is comparing an arrangement before it (for instance, several scattered blocks), to a reference arrangement.

### 3.5. Models for configuration comparison

To tackle this task, we construct from one sample of two configurations two different graphs, one representing each set of objects, in the same way as in the previous experiment. In this section we introduce two architectures that operate on pairs of graphs and that we used to solve the task (an illustration of both architectures is available in the Supplementary Material).

#### 3.5.1. GRAPH EMBEDDING CONDITIONING (GE-GNN)

Let us denote by  $GNN$  a GNN layer, as defined in section 3.3 (note that this layer can either be a message-passing GNN or a RDS). Our first architecture (GE-GNN) uses, at each time step, the graph-level feature  $u_1$  obtained as output of a first GNN,  $GNN_1$ , operating on the first graph. This vector is then concatenated to the second graph-level feature  $u_2$  and thus conditions the computation of a second GNN layer,  $GNN_2$ , operating on the second graph. We then use the second graph-level feature to compute the output. We thus have, for two input graphs  $G_1 = (X_1, A_1, E_1, u_1)$  and  $G_2 = (X_2, A_2, E_2, u_2)$  :

$$\begin{aligned} X'_1, E'_1, u'_1 &\leftarrow GNN_1(X_1, A_1, E_2, u_1) \\ X'_2, E'_2, u'_2 &\leftarrow GNN_2(X_2, A_2, E_2, [u_2 || u'_1]) \end{aligned}$$

As previously, since the outputs have the same dimensions as the inputs, we chain these operations  $N$  times, and at the end we produce the prediction :

$$out \leftarrow MLP_{out}(u'_2)$$

#### 3.5.2. ALTERNATING MODEL (A-GNN)

The GE-GNN model performs sequential computation, with information flowing from the first graph to the second one, which breaks the symmetry of the problem, since the two graphs have a different role in computation. Since it is a

good idea to reproduce the symmetry of the problem in our model, we also present a second model (A-GNN) where the computation is more symmetric and both graphs used play the same role. (maybe introduce an even more symmetric model where every computation is done simultaneously). In this model, we alternate computation on the first graph and on the second graph, by conditioning the computation of  $GNN_1$  by  $u_2$ , and, symmetrically, the computation of  $GNN_2$  by  $u_1$ .

$$\begin{aligned} X'_1, E'_1, u'_1 &\leftarrow GNN_1(X_1, A_1, E_2, [u_1 || u_2]) \\ X'_2, E'_2, u'_2 &\leftarrow GNN_2(X_2, A_2, E_2, [u_2 || u'_1]) \end{aligned}$$

We then use both graph-level features as an input for prediction :

$$out \leftarrow MLP_{out}([u'_2 || u'_1])$$

Note that both these models only use graph embeddings to communicate between graphs, contrary to the Graph Matching Networks of (Li et al., 2019b) that use communication between nodes of the two input graphs directly. In addition to being more computationnally efficient (since we don't have to perform computations over each cross-graph edge), it is a deliberate choice, because further tasks could explore conditioning the computation of a GNN on a graph of objects by other information, such the embedding of a sentence of natural language.

## 4. Experimental Results

In this section, we report the experimental results obtained with our models on our two datasets. For both settings we also provide a generalization analysis and an analysis of the difficulty and easiness of particular configurations in the Supplementary Material.

### 4.1. First Task : Recognizing Configurations

In this section we report the experimental results for the configuration recognition task. Each configuration corresponds to a dataset, for which we generate 10,000 samples, half positive and half negative. We also generate, for each training dataset a distinct test dataset of 5000 samples, coming from the same distribution. Unless specified otherwise, our datasets contain configurations of five objects, although note that our models are completely agnostic to the number of objects. We first compare our models and the baseline on a set of datasets, for which the reference configuration is drawn randomly.

We compare the fully-connected Message-Passing GNN (MPGNN) to the RDS and to a Deep Set baseline. Since we can see the RDS layer as a stripped-down version of the MPGNN layer, namely we have removed the message-computation step between each node and the message-aggregation step, this comparison is effectively a study of

Table 1. Test classification accuracies for the three different models on the simpler configuration recognition task (with 5, 10 and 20 objects). All metrics were computed on 5 different random configurations, to average out the effect of the specific configuration, and 5 different seeds, so 25 training runs total.

MODEL	$n_{obj} = 5$	$n_{obj} = 10$	$n_{obj} = 20$	PARAMETERS
MPGNN	<b>0.98</b> $\pm$ 0.013	<b>0.91</b> $\pm$ 0.013	<b>0.99</b> $\pm$ 0.018	2208
RDS	0.95 $\pm$ 0.025	0.88 $\pm$ 0.041	0.90 $\pm$ 0.083	2038
DEEP SET	0.86 $\pm$ 0.057	0.78 $\pm$ 0.038	0.79 $\pm$ 0.10	2386

Table 2. Test classification accuracies for the three different models on the configuration comparison task. All metrics were computed on 10 different seeds and trained for 5 epochs on each dataset of the curriculum.

ARCHITECTURE AND LAYER	ACCURACY (N=1)	ACCURACY (N=2)	PARAMETERS
GE-GNN (MPGNN)	<b>0.91</b> $\pm$ 0.020	<b>0.93</b> $\pm$ 0.026	4686
A-GNN (MPGNN)	0.90 $\pm$ 0.018	0.92 $\pm$ 0.030	5326
GE-GNN (RDS)	0.64 $\pm$ 0.15	0.65 $\pm$ 0.016	5274
A-GNN (RDS)	0.59 $\pm$ 0.09	0.56 $\pm$ 0.0040	5754
GE-GNN (DS)	0.54 $\pm$ 0.017	0.54 $\pm$ 0.017	4870
A-GNN (DS)	0.55 $\pm$ 0.0080	0.53 $\pm$ 0.013	5190

whether intra-node communication is important for the task at hand as opposed to only letting each node have access to centralized information about the whole configuration. We compare both these settings to a Deep Set (DS) layer, which is also an object-centric model, but that does not explicitly incorporate relational information in its computation: the object features are simply transformed, then aggregated to produce the output. Other baselines could have included MLPs (as are frequently used in object-centric RL settings) or a form of Recurrent Neural Networks (RNNs): however these models do not have built-in invariance to the order of objects. Furthermore, in a setting where the objects come from the output of some perceptive model their order is not guaranteed to be preserved. While this symmetry could in principle be learned from data, the number of permutations explodes very fast with the number of objects  $n$ , and even in our setting with small  $n$  would slow down learning by at least two orders of magnitude.

Table 1 gives the test accuracies of the three different layers. For simplicity, we endow each MLP used in the message computation, node-wise aggregation, graph-wise aggregation and prediction steps with the same number of hidden layers  $d$  and the same number of hidden units  $h$ . Since the DS and RDS layer can be seen as stripped-down versions of the MPGNN layer, if  $d$  and  $h$  stay constant the number of parameters drops for the RDS layer, and drops even further for the DS layer. To allow for a fair comparison with roughly the same number of parameters in each model, we use  $h = 16$  for all architectures and  $d = 1$  for the MPGNN,  $d = 2$  for the RDS and  $d = 4$  for the DS, and we report the number of parameters in the table. For this experiment we report scores with the number of computation runs in each

GNN  $N = 1$  and  $N = 2$ , and see it gives similar results. We train for 20 epochs with the Adam optimizer (Kingma & Ba, 2014), with a learning rate of  $10^{-3}$ . We see that for this parameter regime the MPGNN performs best, garnering almost-perfect accuracy, closely followed by the RDS layer, suggesting that detailed intra-node communication is not crucial for this task; however the experiment suggests that it is helpful for the model to have information relating to its global state when mapping its node function on the objects.

Additionally, we provide results with configurations of  $n_{obj} = 10$  and  $n_{obj} = 20$  of objects, and we notice two interesting phenomena. First, as the number of objects grows the baseline performance drops, suggesting that Deep Sets struggle to find a meaningful way to summarize information as the number of objects grows large. Second, while the RDS performance drops somewhat for 10 and 20 objects, the performance of the MPGNN layer drops for 10 objects, and then becomes almost perfect for 20 objects. The contrast between the MPGNN performance and the other layer’s performance on 20 objects could be explained by the way we generate our negative examples. Since negative examples are complete re-samplings of every object’s position, there is plenty of evidence for a full message passing architecture to detect a negative, and this is information that gets averaged-out in the centralized computation of the RDS layer. This shows the comparative advantage of MPGNN, at a computational cost, in cases where the number of objects is of the same size or greater than the dimension of the embedding used to summarize the information contained in the configuration - which is of the same size as the object feature (10-dimensional). Additional analysis of the relationship between the embedding sizes and the number of

objects is presented in the supplementary material.

## 4.2. Second Task : Comparing Configurations

We now turn to our second task. We compare our two proposed twin-input architectures, Graph Embedding GNN (GE-GNN) and Alternating GNN (A-GNN), each internally endowed with one of the layers studied in the first setting: MPGNN, RDS and DS. For the DS internal layer, we use the graph features produced by the computation on one set of objects to condition the computation on the other, according to the global flow of information in the GE-GNN and A-GNN respectively.

Learning in this setting is more difficult, leading to a great dependence on the initialization of networks: some seeds converge to a good accuracy, some don't perform above chance. This is due to the presence of rotations in the allowed transformations in the positive examples; a dataset containing only translations and scalings leads to good learning. Note that this rotation problem persists for a simplified setup of  $n = 3$  objects. To alleviate this and carry the optimization process we introduce a curriculum of five datasets, each one with a different range of allowed rotations in the generation process, with the last one spanning all possible rotation angles. As in the previous section, to ensure a fair comparison between models in terms of the number of parameters we provide our RDS and DS layers with deeper MLPs ( $d = 1$  for the MPGNN layers,  $d = 3$  for RDS and DS), and we perform  $N = 2$  computation rounds. We report the results in Table 2.

For this task, which requires our models to adaptatively compute a representation of the pairwise distances of the objects to be able to compare two configurations, we see that having models that explicitly compute the full interactions between each pair of objects is a necessary condition for learning the task. To achieve a general, configuration-invariant method of judging whether one configuration is a translated, scaled and/or rotated version of another one, the simplest method is matching all objects from one configuration to the objects of the other configuration, comparing the pairwise distances between all objects in each configuration, and checking they are the same up to a multiplicative constant. We hypothesize that because of their relational inductive bias the models based on the MPGNN layer can learn to perform this task while the other ones cannot, evidenced by an improvement in accuracy of over 30%. Interestingly enough, the way the information flows from one GNN layer to the other (whether the architecture is GE-GNN or A-GNN) seems to be irrelevant in the final performance of the models, suggesting that the first GNN layer, operating on the first collection of objects, does not benefit from additional feedback from the second one for this particular task. Since the GE-GNN architecture can be extended to the case where the first input

is some other form of data, the fact that an asymmetric form of processing performs as well as an architecture based on feedback is encouraging for extending the tasks presented here.

## 5. Discussion

In this work, we showed that the fully-connected computation of the Message-Passing Graph Neural Network is key to recognizing and comparing spatial configurations of objects. We presented evidence that for the simple task of recognizing individual spatial configurations, layers that allow nodes to have access to information about other nodes are key to achieve good performance, whether this communication is centralized, via conditioning by the graph-level feature as in the RDS, or decentralized, as allowed by the MP-GNN layer. This is true for a small number of objects, however when the number of objects becomes large the comparative advantage of MPGNN is clear. As a contrast, we show that for the harder task of comparing two different configurations in the context of dual-input architectures, allowing all-to-all communication between nodes is key to get any learning at all, as models based on the RDS layer fail to achieve good accuracy. These results further understanding of the role of the inductive biases allowed by GNNs in learning to summarize relational information.

This work opens up further research avenues. First, a natural extension is to work directly with images of 3D scenes containing objects, from which graph structure is extracted using perceptive models (Burgess et al., 2019; Greff et al., 2019; Engelcke et al., 2019). Second, moving in the opposite direction, our work could extend towards greater abstraction, e.g., learning to recognize arrangements (such as faces) irrespective of their individual constituent parts. Third, this work can form the basis of more data efficient reinforcement learning for agents interacting with objects in 2D or 3D space. While previous work uses GNNs for policy and value functions (see e. g. (Hamrick et al., 2018a; Wang et al., 2018)), our models could provide a reward signal, allowing agents to learn complex tasks for which it is hard to construct an oracle (Bahdanau et al., 2019).

## Links

The code, datasets and dataset generators are available at the following address: <https://sites.google.com/view/gnn-spatial-reco/>.

## References

Bahdanau, D., Hill, F., Leike, J., Hughes, E., Kohli, P., and Grefenstette, E. Learning to understand goal specifications by modelling reward. In *International Confer-*



- 
- ence on Learning Representations, 2019. URL <https://openreview.net/forum?id=H1xsSjC9Ym>.
- Battaglia, P. W., Pascanu, R., Lai, M., Rezende, D. J., and Kavukcuoglu, K. Interaction networks for learning about objects, relations and physics. *CoRR*, abs/1612.00222, 2016. URL <http://arxiv.org/abs/1612.00222>.
- Battaglia, P. W., Hamrick, J. B., Bapst, V., Sanchez-Gonzalez, A., Zambaldi, V. F., Malinowski, M., Tacchetti, A., Raposo, D., Santoro, A., Faulkner, R., Gülçehre, Ç., Song, H. F., Ballard, A. J., Gilmer, J., Dahl, G. E., Vaswani, A., Allen, K. R., Nash, C., Langston, V., Dyer, C., Heess, N., Wierstra, D., Kohli, P., Botvinick, M., Vinyals, O., Li, Y., and Pascanu, R. Relational inductive biases, deep learning, and graph networks. *CoRR*, abs/1806.01261, 2018. URL <http://arxiv.org/abs/1806.01261>.
- Bruna, J., Zaremba, W., Szlam, A., and Lecun, Y. Spectral networks and locally connected networks on graphs. In *International Conference on Learning Representations (ICLR2014), CBLIS, April 2014*, 2014.
- Burgess, C. P., Matthey, L., Watters, N., Kabra, R., Higgins, I., Botvinick, M., and Lerchner, A. Monet: Unsupervised scene decomposition and representation, 2019.
- Defferrard, M., Bresson, X., and Vandergheynst, P. Convolutional neural networks on graphs with fast localized spectral filtering. *CoRR*, abs/1606.09375, 2016. URL <http://arxiv.org/abs/1606.09375>.
- Duvenaud, D. K., Maclaurin, D., Iparraguirre, J., Bombarell, R., Hirzel, T., Aspuru-Guzik, A., and Adams, R. P. Convolutional networks on graphs for learning molecular fingerprints. In Cortes, C., Lawrence, N. D., Lee, D. D., Sugiyama, M., and Garnett, R. (eds.), *Advances in Neural Information Processing Systems 28*, pp. 2224–2232. Curran Associates, Inc., 2015. URL <http://papers.nips.cc/paper/5954-convolutional-networks-on-graphs-for-learning-molecular-fingerprints.pdf>.
- Engelcke, M., Kosiorek, A. R., Jones, O. P., and Posner, I. Genesis: Generative scene inference and sampling with object-centric latent representations, 2019.
- Gilmer, J., Schoenholz, S. S., Riley, P. F., Vinyals, O., and Dahl, G. E. Neural message passing for quantum chemistry. *CoRR*, abs/1704.01212, 2017. URL <http://arxiv.org/abs/1704.01212>.
- Gori, M., Monfardini, G., and Scarselli, F. A new model for learning in graph domains. In *Proceedings. 2005 IEEE International Joint Conference on Neural Networks*, 2005., volume 2, pp. 729–734 vol. 2, July 2005. doi: 10.1109/IJCNN.2005.1555942.
- Greff, K., Kaufman, R. L., Kabra, R., Watters, N., Burgess, C., Zoran, D., Matthey, L., Botvinick, M., and Lerchner, A. Multi-object representation learning with iterative variational inference, 2019.
- Hamrick, J. B., Allen, K. R., Bapst, V., Zhu, T., McKee, K. R., Tenenbaum, J. B., and Battaglia, P. W. Relational inductive bias for physical construction in humans and machines. *CoRR*, abs/1806.01203, 2018a. URL <http://arxiv.org/abs/1806.01203>.
- Hamrick, J. B., Allen, K. R., Bapst, V., Zhu, T., McKee, K. R., Tenenbaum, J. B., and Battaglia, P. W. Relational inductive bias for physical construction in humans and machines, 2018b.
- Hudson, D. A. and Manning, C. D. Learning by abstraction: The neural state machine, 2019.
- Johnson, J., Krishna, R., Stark, M., Li, L., Shamma, D. A., Bernstein, M. S., and Fei-Fei, L. Image retrieval using scene graphs. In *2015 IEEE Conference on Computer Vision and Pattern Recognition (CVPR)*, pp. 3668–3678, June 2015. doi: 10.1109/CVPR.2015.7298990.
- Keriven, N. and Peyré, G. Universal invariant and equivariant graph neural networks. *CoRR*, abs/1905.04943, 2019. URL <http://arxiv.org/abs/1905.04943>.
- Kingma, D. P. and Ba, J. Adam: A method for stochastic optimization, 2014.
- Kipf, T., van der Pol, E., and Welling, M. Contrastive learning of structured world models, 2019.
- Kipf, T. N. and Welling, M. Semi-supervised classification with graph convolutional networks. *CoRR*, abs/1609.02907, 2016. URL <http://arxiv.org/abs/1609.02907>.
- Krishna, R., Zhu, Y., Groth, O., Johnson, J., Hata, K., Kravitz, J., Chen, S., Kalantidis, Y., Li, L., Shamma, D. A., Bernstein, M. S., and Li, F. Visual genome: Connecting language and vision using crowdsourced dense image annotations. *CoRR*, abs/1602.07332, 2016. URL <http://arxiv.org/abs/1602.07332>.
- Lake, B. M., Ullman, T. D., Tenenbaum, J. B., and Gershman, S. J. Building machines that learn and think like people. *Behavioral and Brain Sciences*, 40, Nov 2016. ISSN 1469-1825. doi: 10.1017/S0140525X16001837. URL <http://dx.doi.org/10.1017/S0140525X16001837>.

- 
- Li, R., Jabri, A., Darrell, T., and Agrawal, P. Towards practical multi-object manipulation using relational reinforcement learning, 2019a.
- Li, Y., Gu, C., Dullien, T., Vinyals, O., and Kohli, P. Graph matching networks for learning the similarity of graph structured objects. *CoRR*, abs/1904.12787, 2019b. URL <http://arxiv.org/abs/1904.12787>.
- Ma, G., Ahmed, N. K., Willke, T. L., and Yu, P. S. Deep graph similarity learning: A survey, 2019.
- Maron, H., Fetaya, E., Segol, N., and Lipman, Y. On the universality of invariant networks. *CoRR*, abs/1901.09342, 2019. URL <http://arxiv.org/abs/1901.09342>.
- Maurer, D., Grand, R. L., and Mondloch, C. J. The many faces of configural processing. *Trends in Cognitive Sciences*, 6(6):255 – 260, 2002. ISSN 1364-6613. doi: [https://doi.org/10.1016/S1364-6613\(02\)01903-4](https://doi.org/10.1016/S1364-6613(02)01903-4). URL <http://www.sciencedirect.com/science/article/pii/S1364661302019034>.
- Norcliffe-Brown, W., Vafeias, E., and Parisot, S. Learning conditioned graph structures for interpretable visual question answering. *CoRR*, abs/1806.07243, 2018. URL <http://arxiv.org/abs/1806.07243>.
- Pylyshyn, Z. W. *Things and places: How the mind connects with the world*. MIT press, 2007.
- Santoro, A., Raposo, D., Barrett, D. G., Malinowski, M., Pascanu, R., Battaglia, P., and Lillicrap, T. A simple neural network module for relational reasoning. In Guyon, I., Luxburg, U. V., Bengio, S., Wallach, H., Fergus, R., Vishwanathan, S., and Garnett, R. (eds.), *Advances in Neural Information Processing Systems 30*, pp. 4967–4976. Curran Associates, Inc., 2017. URL <http://papers.nips.cc/paper/7082-a-simple-neural-network-module-for-relational-reasoning.pdf>.
- Scarselli, F., Gori, M., Tsoi, A. C., Hagenbuchner, M., and Monfardini, G. The graph neural network model. *IEEE Transactions on Neural Networks*, 20(1):61–80, Jan 2009. ISSN 1941-0093. doi: 10.1109/TNN.2008.2005605.
- Sieb, M., Zhou, X., Huang, A., Kroemer, O., and Fragkiadaki, K. Graph-structured visual imitation. *CoRR*, abs/1907.05518, 2019. URL <http://arxiv.org/abs/1907.05518>.
- Teney, D., Liu, L., and van den Hengel, A. Graph-structured representations for visual question answering. *CoRR*, abs/1609.05600, 2016. URL <http://arxiv.org/abs/1609.05600>.
- Wang, T., Liao, R., Ba, J., and Fidler, S. Nervenet: Learning structured policy with graph neural networks. In *International Conference on Learning Representations*, 2018. URL <https://openreview.net/forum?id=S1sqHMZCb>.
- Xu, K., Hu, W., Leskovec, J., and Jegelka, S. How powerful are graph neural networks? *CoRR*, abs/1810.00826, 2018. URL <http://arxiv.org/abs/1810.00826>.
- Zaheer, M., Kottur, S., Ravanbakhsh, S., Poczos, B., Salakhutdinov, R., and Smola, A. Deep sets, 2017.

# Supplementary Material

## 1. Visual illustration of our layers and architectures

In this section we provide an illustration of the two architectures used in this work (Figure 1) and of the three layers used in this work (Figure 2, on the next page).

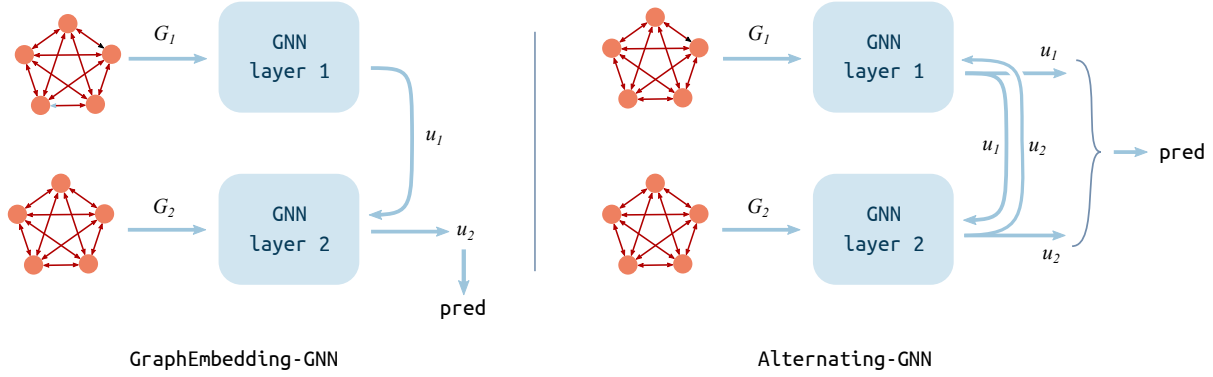


Figure 1. An illustration of the two dual-input architectures used in this work for the configuration comparison task. The GraphEmbedding-GNN uses directed computation, first operating on one graph then using the resulting embedding to condition the computation on a second graph, with no feedback; the Alternating-GNN proceeds the same way at first, and the embedding of the second graph is fed back to condition the computation of the first graph. GE-GNN only uses the output of the second GNN layer for prediction; whereas A-GNN concatenates both output embeddings and uses the resulting vector as a basis for prediction.

## 2. Model Heatmaps

In this section, we are interested in visualizing how the model’s prediction function varies with the change in position of one object, while all others are held constant. Since we output for each model and input configuration scores for the positive  $s_{pos}$  and negative  $s_{neg}$  classes, we can use their difference  $D = s_{pos} - s_{neg}$  as a synthetic, non-discrete metric for quantifying how confidently the model predicts an input corresponds to the positive (resp. negative) classes for positive  $D$  (resp. negative  $D$ ). The  $D = 0$  level corresponds to the boundary between the positive and negative classes.

The study of how  $D$  varies with the perturbation of a single object’s position is of great interest, for several reasons. First it is interesting in the context of using a model, trained on a configuration recognition task, to inform an agent trying to reproduce a given arrangement of objects given an environment filled with the right objects at arbitrary positions. In this context, a realistic agent would be able to move only one object at a time, and the learned configuration recognition model should provide a useful signal under change of individual object’s position (one could use gradient ascent of  $D$ , or use the predicted output class as a learned reward function in an RL setting). Second, since we provide as a training dataset only samples that have been globally transformed (translation/scaling/rotation of *all* objects, resampling of *all* object position), it of general interest to examine how this training regime based on global transformations translates when the transformations performed are only local, eg. moving only one object.

### 2.1. Configuration Recognition

To visualize the variation of  $D$  for a given model, we plot the position of the five objects composing the configuration in the 2d plane as colored dots. We fix four of these objects, represented as dark blue dots, and move the fifth one on a 2d grid. For each point on the grid we compute  $D$  and we color the corresponding pixel in our map. Note that we clamp values smaller

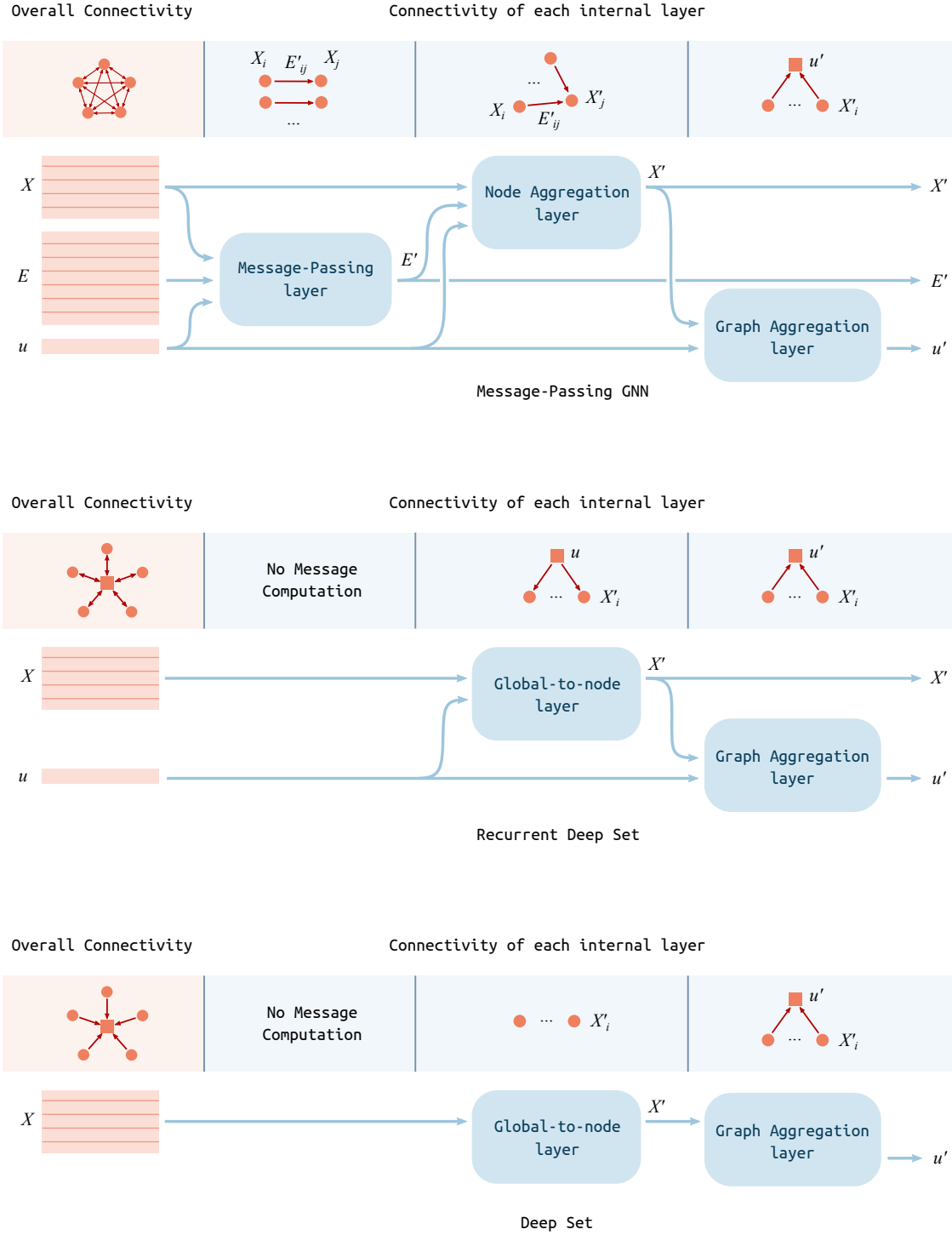


Figure 2. An illustration of the three different layers used in this work. Going from MPGNN to RDS to DS can be seen as an ablation study, where different elements are withdrawn from the layer to study their impact on final performance. For the MPGNN and RDS layers, the output tensors are then fed back as inputs of the model, providing recurrent computation; this is not the case for the Deep Set layer. In this figure, emphasis is put on the connectivity implied by each layer. Nodes are represented by orange disks, the graph-level embedding, which can be seen as a special kind of node, is represented with an orange square. From top to bottom, we go from all-to-all connectivity to bidirectional all-to-one to unidirectional all-to-one.

than  $-5$  and greater than  $5$  to keep a mostly uniform color scale. The parameters are the same as the ones used in the main text. We visualize the resulting heatmaps in Figure 3.

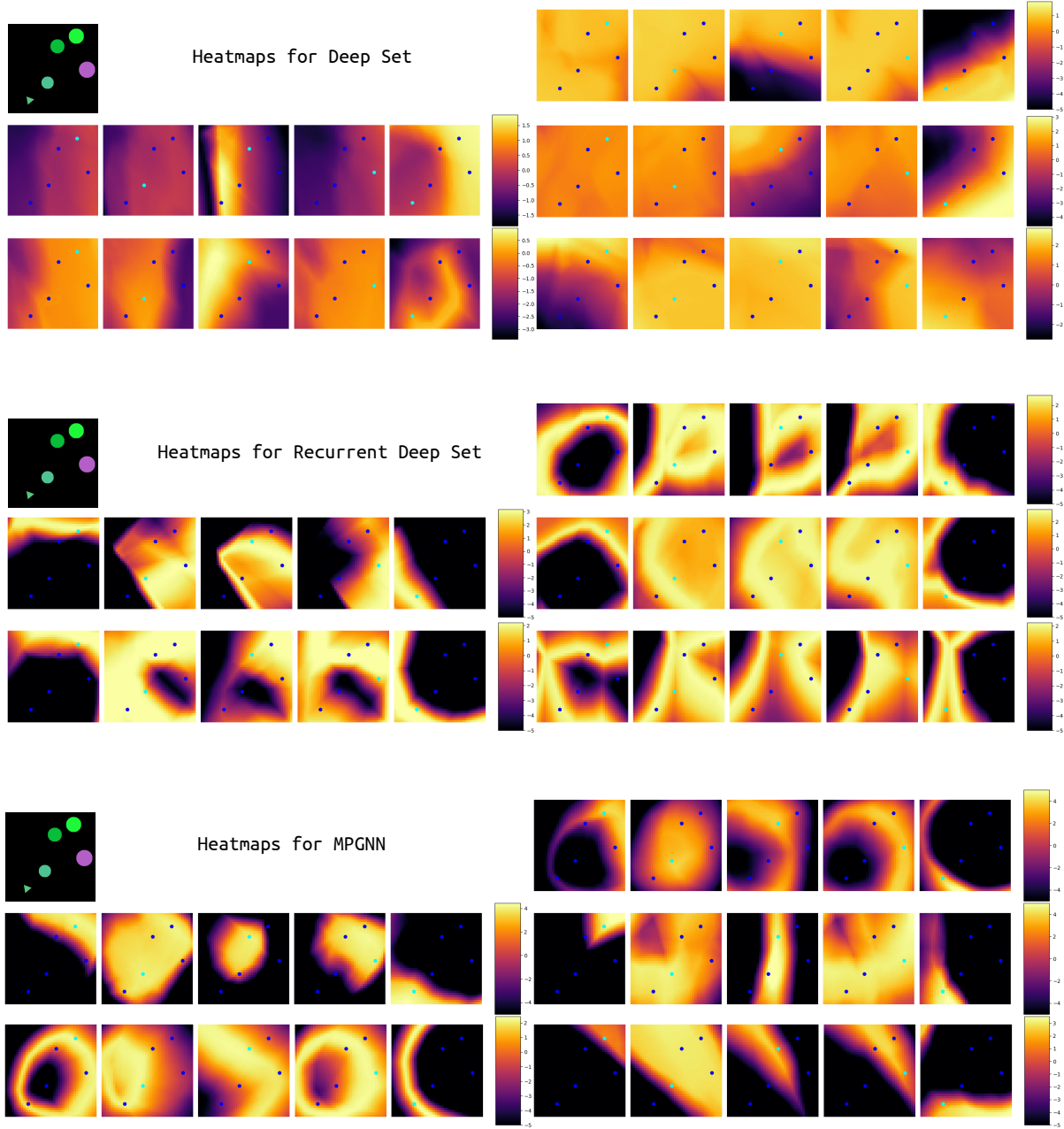


Figure 3. Heatmaps for all seeds of our three layers. The configuration the models were trained to recognize is given at the top left of each figure. Each image represents the variation of the score difference  $D$  with the change of position of the object represented in cyan. Each row gives this variation with the movement of a different object. Each row corresponds to one trained seed, we show several seeds to illustrate the variation in the final model induced by change in initialization and order of presentation of data.

A first glance at Figure 3 already shows us several things. The functions learned by the different instances of Deep Set are of qualitatively lower quality than the ones learned by the seeds of RDS and MPGNN: most Deep Sets manifest complete invariance to the change in position of all but one or two objects, which seems unhelpful in learning to disambiguate positive and negative examples. Furthermore, when the models do exhibit variation in the scores for movement of one object, these

variations seem arbitrary and do not depend strongly on the positions of the other objects, and the original position of the cyan object is rarely if ever at a local maximum of  $D$ . This suggests that if one were to attempt a gradient ascent of  $D$  with respect to each object’s position to reconstitute the original configuration one would never attain it, since the original position itself does not lie at a maximum.

Now looking at the heatmaps of the seeds of the Recurrent Deep Sets, the functions learned by these models seem more expressive, exhibiting greater variation that depend of the fixed objects’ positions in 2d space. The moved objects lie more often at a high point of  $D$ , and the models are never invariant to the movement of an individual object. The higher points of  $D$  manifest themselves as crests, which seem somewhat localized for objects near the center of the configuration, and that go around the other objects for objects farther away from the center of the configuration. The first and last heatmaps of each row are quite eloquent: the models seem to have learned that the cyan object must lie at a certain distance of the center of the configuration, irrespective of its angle with the rest of the objects, giving rise to great circular regions of a low  $D$  value surrounded by a ring-like crest of high  $D$ .

Finally, the heatmaps of the Message-passing GNNs seem qualitatively similar to the ones of the Recurrent Deep Sets, albeit somewhat smoother. In this case we also seem to have some more cases of well-behaved score function, where the value is high in a small localized region around the original position of the object and low everywhere else (see for instance the second object of the top-left row, or the first object of the middle-right row). A difference we can note with the RDS is that, although we find the same ring-shaped crests for the peripheral objects, the rings seem more oriented than in the previous setting (see for instance the first and last object of the top-right row). We will find a stronger version of this behavior in the comparison setting.

As a last general remark, we remind the reader that because the model maps the same learnable function on nodes/edges ( $MLP_X$  and  $MLP_E$  in the main text), the functions the GNN learns must be informative for all objects. While this confers the model ability to learn and generalize on variable numbers of objects with the same number of parameters, it also makes the task more difficult since each object may play a different role in the configuration, and the model could benefit from learning different functions for each of them. We see from the preceding heatmaps that the RDS and MPGNN models nevertheless manage to learn functions flexible enough to be able to adapt to changes in the position of a central object vs a peripheral object.

## 2.2. Configuration Comparison

We perform the same kind of visualization experiment for the models trained to compare two configurations. This time, since the models are universal, we generate a new random configuration of five objects, and ask the model to compare it to a copied version where we move only one object on the grid, in a similar fashion to the previous section. We also clip the values of  $D$  to  $[-5; 5]$  to keep similar color scales across seeds. We show heatmaps for one random draw of configuration, across seeds, in Figure 4. The parameters used are the same as the ones in the main text, with  $N = 2$ .

First, we can remark that the Alternating-GNN architecture, coupled with the RDS layer fails to learn any position-dependent function, at least when moving any single object. However, when the same RDS layers are used with the GraphEmbedding-GNN architecture the picture is relatively different. The regions of high- $D$  are, in 4 out of 5 cases, similar versions of rings centered around a central position, close to the geometrical center of the configuration. This strongly suggests that the model learns to compare each node’s position to the center of the configuration, which is made possible by the fact that the node model inside the layer has access to the global vector  $u$ . What is more remarkable is that each node ‘gets it right’ and is able to compute the difference between its distance to the center in the first vs in the second graph, based only on the information contained in the first graph’s embedding. We can also note that the A-GNN architecture is an extension of the GE-GNN one, so the flow of information of the second one could in principle be reproduced in the first one, and the two models should be able to learn similar functions. However, the comparison between A-GNN and GE-GNN suggests that in the RDS case the optimization process is less favorable for the A-GNN architecture.

Second, when replacing RDS layers with MPGNNs, the heatmaps change completely, reflecting the changes in learned functions that are also evidenced by the notable increase in accuracy of those models. While the heatmaps of those models sometimes share the ring-like structure learned by GE-GNN (RDS), often those rings are interrupted by regions of low score difference (particularly visible in the bottom-left row for both models). A very interesting feature of this interruption is that it seems to follow the principal direction of the set of positions of the other objects, allowing the model to produce a small, localized region of high  $D$  around each object. This effect is also smaller when there is no clear principal direction, or when the object is close to the center of the configuration. This suggests that the model learns to use the information of

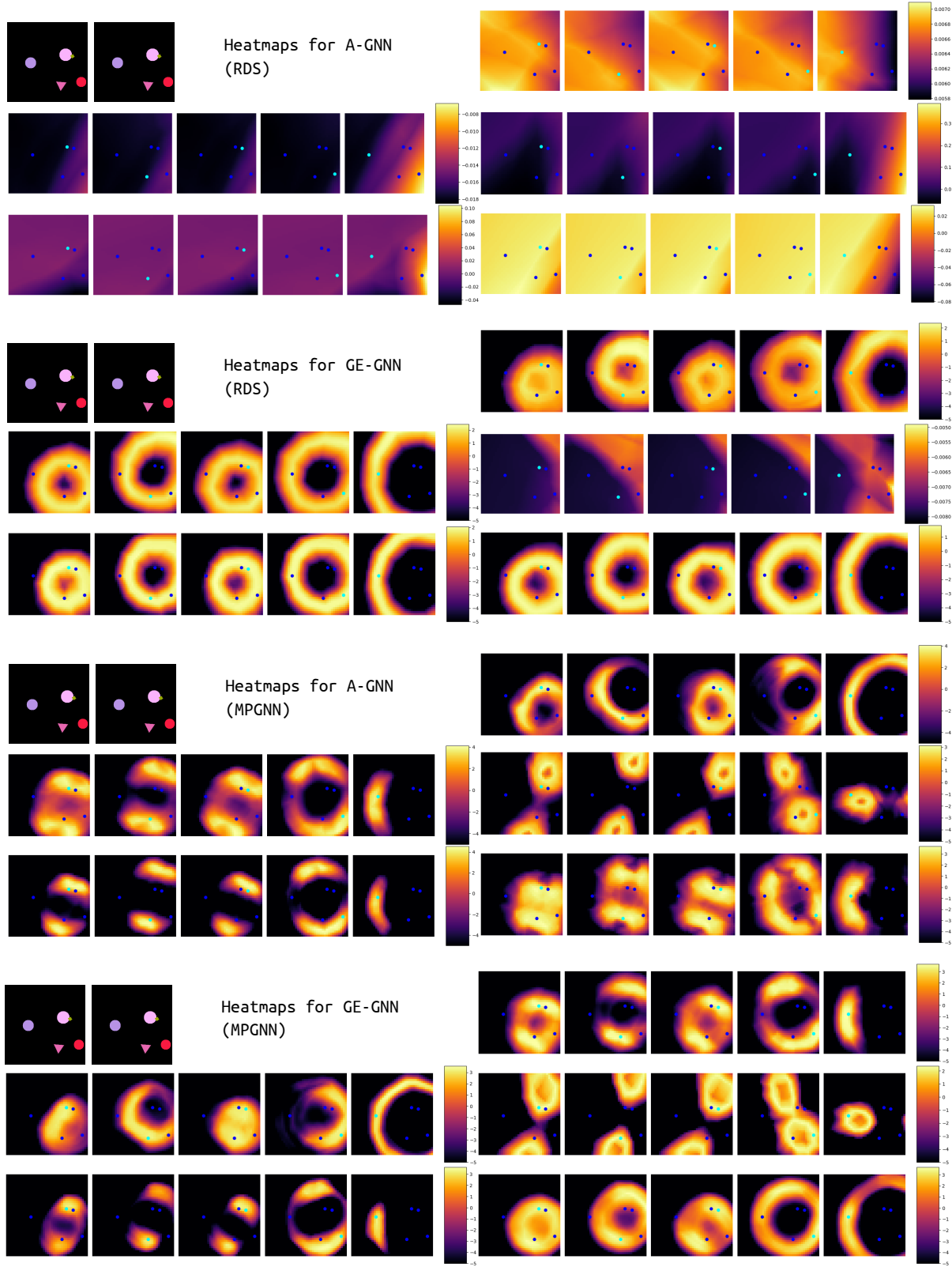


Figure 4. Heatmaps for five seeds of our layer-architecture combination. We left out all DS-based models, because the learned functions are quasi-constant for all objects. We symbolize the fact that the model actually has to compare configurations by displaying two versions of the randomly sampled test configurations at the top left corner of each sub-figure.



the distance of each object to the geometrical center of the configuration, but also of the relation between each individual object and the alignment of all the others; this is specifically made possible by the MPGNN’s relational computation, since it makes available to each node a summary of information computed based on the features of the other nodes. An interesting side-effect of this learned function is that it has an unexpected kind of symmetry, and we find symmetrical regions of high  $D$  values on each side of the axis of alignment of the other objects. Presumably this effect would fade if we explicitly included reflections as negative samples, and the models would learn to also consider information about which side of the axis the object is on. Interestingly, and as a contrast to the RDS case, both architectures learn similar functions, suggesting that the effect of good structure inside the layer is stronger than the effect of higher-level information passing for learning this particular task (as can be seen from the middle-right row, where the same initialization and training produce very similar heatmaps for both architectures).

Finally, we can also note that because this setting is more general, in the sense that the model must learn prediction functions that apply to any configuration, the learned functions seem much more systematic than in the configuration recognition case.

As a conclusion to this visualization experiment, we can get a sense of how the inductive biases of the different layers we consider in this work influence the expressivity of our models for learning to recognize and compare spatial configuration of objects. Because each node in the RDS layers only has access to information pertaining to the configuration as a whole and to itself, it only learns a function that is invariant to rotations of object positions around the geometrical center of the configuration. Because the MPGNN layer allows each node to have access directly to the other nodes’ information, it is able to compute refined functions with more complex symmetries.

### 3. Easier and Harder Datasets to Recognize

In this section, we are interested, in the context of the configuration recognition task, in studying how particular configurations may be harder or easier to recognize for our models. We hypothesise that more regular arrangements of objects must be easier to tell apart than more random configurations, and that configurations with a high degree of object diversity (many colors, many shapes) must also be easier to learn to classify, because the models can more easily identify and match the different objects. To test this, we compare one randomly generated dataset (regular difficulty) with 1) a configuration where all objects are red circles of the same size positioned at the same point; 2) a configuration where all the objects are red circles of the same size arranged in a line; 3) a configuration where all the objects are randomly positioned red circles of the same size; and 4) the same configuration as 3), but with circles of varying color. We train our three layers, DS, RDS and MPGNN, to recognize these configurations, and report the results in Figure 5, along with an illustration of the configurations.

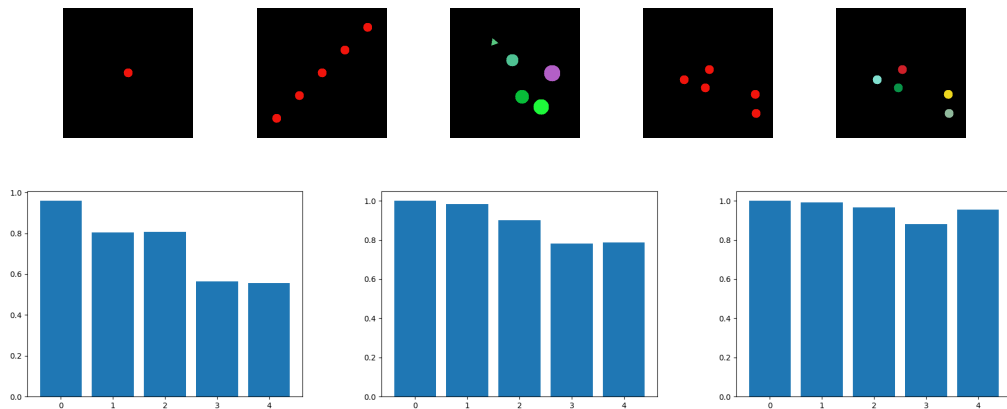


Figure 5. The top row represents the configurations we trained our models with, as described in the text. The bottom row is a bar plot of the final test accuracy of (from left to right) the Deep Set, Recurrent Deep Set and Message-Passing GNN on each of the 5 datasets, in the order specified in the top row (results were computed on 5 seeds for each dataset).

We interpret the results as follows : the fourth configuration, the one with all red circles, does seem to be more difficult to learn across all models. This may be due to the intrinsic hardness of the task on this configuration, or to the fact that randomly resampled positions for the negative examples of this dataset may give with non-negligible probability configurations that are close to a translated/rotated version of the reference example, because any object can be identified with any other. This



second option may translate into negative examples that may resemble strongly positive examples, confusing the model. Interestingly, the problem fades when we identify each object by giving it a color, suggesting this second explanation is correct, but only for the MPGNN. For MPGNN, performance is roughly similar on all the other datasets. However, for DS and RDS, there seems to be considerable difference between datasets. The DS layer fails to perform significantly above chance for both right-hand configurations, suggesting arrangements of similar objects are difficult for this kind of model. Interestingly, the DS layer performs similarly on the aligned red circles than on the random diverse configuration, but significantly better than on the configuration with randomly scattered red circles, suggesting it is able to use the alignment information to reach above-chance accuracy, but not in a completely reliable way. As a contrast, the RDS layer performs near-perfectly on this configuration, showing that the additional connectivity of the RDS helps it in discovering exploitable regularities in the data.

## 4. Higher number of objects

In this section, we present results, in the configuration comparison setting, when we augment the number of objects. First we present results for training on 10 and 20 objects for our MPGNN-based architectures, then we perform a generalization study, where we train our models on 5 objects and test them on number of objects ranging from 4 to 20.

### 4.1. Training on higher number of objects

We keep the same training settings (hyperparameters, curriculum of available rotation angles) as in the experiment presented in the main text. We present the results of this new experiments in Table

Table 1. Test classification accuracies for the different models on the configuration recognition task, with higher number of objects. All metrics were computed on 10 different seeds for each case.

ARCHITECTURE AND LAYER	10 OBJECTS	20 OBJECTS
GE-GNN (MPGNN)	$0.88 \pm 0.033$	$0.7 \pm 0.20$
A-GNN (MPGNN)	$\mathbf{0.91} \pm 0.021$	$\mathbf{0.78} \pm 0.184$
GE-GNN (RDS)	$0.80 \pm 0.14$	$0.51 \pm 0.016$
A-GNN (RDS)	$0.66 \pm 0.15$	$0.56 \pm 0.0040$
GE-GNN (DS)	$0.50 \pm 0.0030$	$0.50 \pm 0.0020$
A-GNN (DS)	$0.50 \pm 0.0040$	$0.50 \pm 0.0010$

We see that our MPGNN models, with fixed hyperparameters, are able to scale to configurations of a higher number of objects. In our experiments, the size of the graph embedding, used to pass information from one graph to the next, is  $d = 10$ . We notice that for  $n_{obj} = 20$  objects ( $n_{obj} < d$ , a fact that imposes a bottleneck on the amount of information that is able to pass from one GNN layer to the other) performance decreases. Looking at the histogram of test accuracies reveals that a good proportion of seeds achieve around 0.90 accuracy, and the overall score is brought down by a few seeds who do not manage to achieve above-chance accuracy. Learning a good function is still possible in this setting, but the optimization process becomes more sensitive to the quality of the initial conditions.

### 4.2. Generalizing to a higher number of objects

In this section we train our MPGNN models on  $n_{obj} = 5$  objects and test them on datasets of couples of configurations ranging from  $n_{obj} = 4$  to  $n_{obj} = 20$ . We report the findings in Figure 6.

On the plot, we can clearly identify  $n_{obj} = 5$ , the training number of objects. We see both our architectures exhibit very little generalization capability for different number of objects, and do not perform above chance for  $n_{obj} > 8$ . This suggests that the functions learned by our models are not useful when the number of objects get too large: for instance, the fact that the GNN layers learn to estimate their distance to the center of the comparison (see Section 2) may not be as useful when there are many objects with a similar distance to the geometrical center of the configuration. Presumably, training on datasets with a range of possible  $n_{obj}$  instead of just one could help to alleviate this problem.

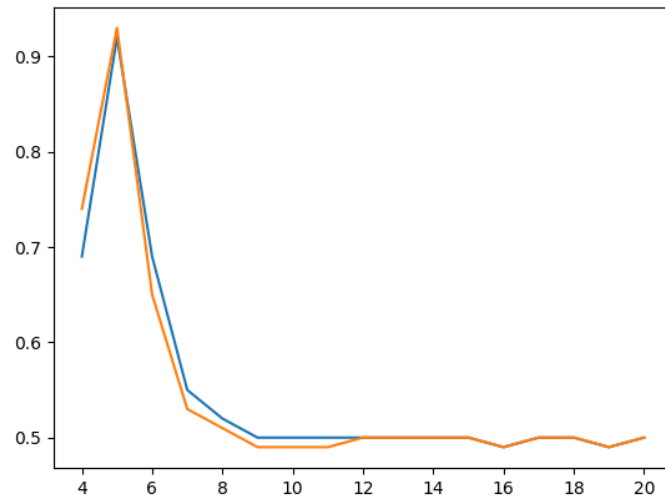


Figure 6. Test accuracies for testing datasets with number of objects ranging from 4 to 20, represented on the x-axis. The blue curve corresponds to A-GNN (MPGNN), and the orange curve corresponds to GE-GNN (MPGNN).